Supplementary Information for

Cytokinetic abscission is part of the mid-blastula transition in early zebrafish embryogenesis

Shai Adar-Levor, Dikla Nachmias, Shani T. Gal-Oz, Yarden M. Jahn, Nadine Peyrieras, Assaf Zaritsky, Ramon Y. Birnbaum*, Natalie Elia*

Natalie Elia: elianat@post.bgu.ac.il

Ramon Y. Birnbaum: ramonb@bgu.ac.il

This PDF file includes:

Other supplementary materials for this manuscript include the following:

Movies S1 to S8

Supplementary methods

Fish maintenance

The animal work performed in this study was approved by the Ben Gurion University Institutional Animal Care and Use Committee (BGU520916). AB wild type zebrafish were maintained and bred at 28 °C according to standard protocols.

mRNA and morpholino

Cep55l, Tsg101, Chmp4bb, Chmp4ba zebrafish (*Danio rerio*) coding sequences were amplified by PCR from zebrafish cDNA using specific primers (Table S1) and sub-cloned into mCherry-C1 vector (Clontech, Mountain View, CA). hVPS4A and hVPS4^{EQ} in pEGFP-C1 were previously described in Elia et. al. (1) All plasmids then subcloned into pCS2+ vector (kindly provided by Gil Levkowitz, Weizmann Institute of Science, Israel). eGFP-FRB-CAAX was also sub cloned into pCS2+ vector. mRNA encoding for mCherry-cep55 mCherry-tsg101, mCherry-chmp4bb, mCherry-chmp4ba, GFP-VPS4, GFP-VPS4^{EQ} and GFP-CAAX were generated by *in-vitro* transcribed using mMessage mMachine SP6 kit (AM-1340 Invitrogen) and purified using RNeasy mini kit (74104 Qiagen). Morpholino oligos against chmp4bb and standard control oligos (Gene Tools, Inc.) were designed and managed according to manufacture protocol (Table S1). Two morpholino oligos were injected and analyzed by western blot analysis for chmp4bb knock down (MO_1chmp4bb and MO_2chmp4bb) (Fig. S4*D*). MO_1chmp4bb was found to be more efficient by western blot analysis, and was therefore used in all the presented experiments.

Embryos microinjection and mounting for live imaging

mRNA (0.8ng-1ng) or morpholino oligos (5ng) were microinjected into wild type embryos at one-cell stage together with 1.3 ng HiLyte Fluor™ 488-Tubulin (TL488M, Cytoskeleton, Inc.) or 1.3 ng TAMRA Rhodamine Tubulin (TL590M, Cytoskeleton, Inc.) and 0.1% phenol red (P0290, Sigma-Aldrich) using microinjector (World Precision Instrument, Sarasota, FL) and kept in Danieau buffer (DBx1) (174 mM NaCl, 21 mM KCl, 12 mM MgSO4, 18 mM Ca(NO3)2, 15 mM HEPES). Under these conditions, embryos were viable and showed normal cell division and physiological morphology at blastula stage (Fig. 1*B*, Fig. S1*B*). Injected embryos were dechorionized using fine tweezers and placed in specialized agar chambers for imaging.

Preparation of agar chambers: specialized agar wells designed for mounting zebrafish embryos at blastula stage for live imaging were prepared according to Whur et. al (2). In short, a mold with 8 wells, each 0.6-0.7 μm^2, was placed in a 35 mm glass bottom µ-dish (81156, ibidi) (Fig S1*A*). Wells were mounted by pouring 1 ml of 2.5% melted agarose (50080, Lonza Rockland, ME in Danieau buffer (DBx1) into the µ-dish with the mold inside. After agar solidifying, the mold was carefully removed and dechorionized embryos were inserted to the chamber with the animal pole facing the coverslip and covered with DBx1 (Fig 1*A*).

Whole-mount immunostaining

Naïve embryos and injected embryos with GFP-VPS4^{EQ}, at 2-2.75 hpf (7^{th}-9^{th} cell cycles, 128-512 cells) and at 3.5-4.5 hpf (11^{th}-12^{th} cell cycles) were fixed (4% PFA, overnight at 4°C), washed twice in PBS supplemented with 0.1% Tween20, dechorionized with fine tweezers and placed in a 24-well dish coated with 1% agar. Embryos were then permeabilized in 0.25% trypsin-EDTA (Biological industries, Israel) in Hank's balanced salt solution (Thermo Fisher Scientific, Waltham, MA) for 10 minutes on ice, washed three times for 30 minutes in washing buffer (PBS plus 0.2% Triton X-100) and post-fixed with 4% PFA for 1 hour at room temperature. Embryos were blocked for 2 h at room temperature in blocking solution (10% fetal bovine serum, 1% BSA and 0.2% Triton X-100 in PBS) and incubated with monoclonal anti α-Tubulin (DM1A; Sigma-Aldrich, 1:1000, overnight). After washing (x3, 20 minutes) embryos were incubated with a secondary antibody Alexa Flour 488 anti-mouse (A21202, Invitrogen, 1:1000, overnight) and washed again (x3, 20 minutes). Finally, embryos were stained with Hoechst 1:1000 (H-3570 Invitrogen) for 30 minutes, washed (x2, 15 minutes) and kept in 25% glycerol in PBS. For dissection, embryos were placed on a microscope slide in 50% glycerol solution and the yolk was cut out using a sharp scalpel and tweezers. Last, embryos were mounted in fluoromount-G® (SouthernBiotech, Birmingham, AL) on a coverslip with the animal pole facing the coverslip. Samples were imaged by confocal microscopy as described below.

Click-iT labeling of transcription pattern

Click-iT® reaction kit was used to visualize transcription levels as previously described by Chan et al. 2019 (3). One-cell-stage embryos were microinjected with 50 pmols of 5-ethynyl uridine (5-EU, E10345), and 0.1% phenol red and kept in DBx1. Depending on the desired

developmental stage, injected embryos were fixed 2-5 hpf (with 3% PFA and 0.1% glutaraldehyde mixture (overnight, 4°C) and washed three times with PBSx1. Next, embryos were then dechorionized with fine tweezers and placed in a 24-well dish coated with 1% agar for immunostaining and click-it reaction.

Immunostaining for 5-EU injected embryos: embryos were permeabilized with PBS with 0.5% Triton X-100 (PBS-T) at room temperature for 30 minutes, followed by dehydration with serial dilutions of methanol in PBS-T (25%,50%,75%,100%) for 5 minutes in each dilution. Dehydrated embryos were incubated in 100% methanol (-20°C, 2 hours) and subjected to rehydration with serial methanol in PBS-T (75%,50%,25%, 0%). Embryos were then washed, blocked (0.2% Triton X-100, 1%BSA, 10% fetal bovine serum in PBS) for 2 hours in room temperature and stained with anti α-Tubulin (DM1A; Sigma-Aldrich, 1:1000, overnight) followed by secondary antibody staining (Alexa Flour 488 anti-mouse 1:1000,2 hours in room temperature).

Click-iT reaction: embryos were incubated for 1 hour at room temperature in cell reaction mix: 5 μM of Alexa Fluor® 594 azide (A10270) in Click-iT reaction buffer according to manufacture protocol (Click-iT® reaction buffer kit C10269, Invitrogen). Embryos were washed twice for 10 minutes in PBS solution with 2% BSA. Finally, embryos were stained with Hoechst (0.5 hour, 1:1000), dissected and mounted as described above.

Analysis of transcription pattern similarities in connected and non-connected cells

The agreement in transcription patterns between adjacent cells was quantified using montage images of embryos labeled with 5-EU and stained with Tubulin, as described above. First, clusters of cells connected by intercellular bridges were annotated according to Tubulin staining in specific regions in the embryos that exhibited high levels of heterogeneity in cellular transcription patterns. Next, a transcription pattern was manually assigned to cells in in the selected regions according to their 5-EU staining (Fig. 5*B*). Then the transcription agreement probability matrix was plotted for cells connected by intercellular bridges (A, A'), and for neighboring cells that are not connected by a bridge (A, B) (Fig. 5*F*). Each bin in the column (c) and row (r) holds the fraction of cell pairs where one cell had transcription pattern c and the other transcription pattern r (i.e. the accumulated values in the matrix sum up to 1). For example, in Fig. 5 the bin at the column labeled "no" and the row labeled "high" holds the fraction of cell pair with the corresponding transcription patterns. Note, that these matrices were not completely asymmetric, (i.e. the value in bin (c,r) could slightly deviated from the value in

bin (r,c) because the selection of A-A' and A-B pairs used a common "anchor" A (see illustration in Fig. 5*E*). The disagreement between the asymmetric matrix entries was small, would converge to 0 with larger N - sampling of pairs, and did not affect the interpretation of the results in any way. The accumulated diagonal bins of these transcription agreement probability matrices held the overall fraction of adjacent cell pairs with agreement in their transcriptional patterns.

To assess the transcription agreement in cell clusters (Fig. 5*G*), we implemented a simplistic simulation to calculate the expected agreement in cell clusters under the assumption of no spatial independence in transcriptional patterns. For clusters of size 2, 3, or 4, we selected 100,000 cell clusters using the observed transcriptional pattern marginal distribution (Fig. 5*D*) and recorded the fraction of homogeneous clusters – where all cells had the same transcriptional pattern. We compared these simplistic predicted probabilities to the matching probabilities recorded in experiments (Fig. 5*G*).

RNA-seq data and visualization

RNA sequencing expression data (FPKM) of zebrafish embryos was downloaded from the Expression Atlas site (https://www.ebi.ac.uk/gxa/experiments/E-ERAD-475) (4). Eight developmental stages (zygote, cleavage 2 cell, blastula 128 cell, blastula 1k cell, blastula dome, gastrula 50% epiboly, gastrula shield, gastrula 75% epiboly) were used for the analysis. Normalized FPKM values that were lower than one was replaced by one, and all values were log2 transformed. Only the set of abscission related genes that were expressed (above zero) in at least 3 of the 8 samples were considered (48 genes). Hierarchical gene clustering was performed with hclust R function ("complete" method), using the normalized log2-transformed FPKM values of the eight developmental stages. Clusters were sorted manually and genes within clusters were sorted according to their scaled expression in the Zygote stage. For heatmaps presentation, the log2-transformed FPKM expression values of the presented genes were standardized by subtraction of each gene's mean expression, followed by division by the standard deviation across all samples. Cyclin d1, a well-established zygotic gene was used as a positive control in our analysis was clustered into a singleton cluster and is presented in the first row of the heatmaps.

Photoactivation

Embryos were injected with 0.5 ng of Photoactivated-mCherry (PA-mCherry) and 1.3 ng HiLyte 488-Tubulin, dechorionated and mounted for live imaging as described in main methods. At 16-cells stage, embryos were imaged at sec intervals for 4 minutes using on a fully incubated confocal spinning-disk microscope at 26 °C (Marianas; Intelligent Imaging, Denver, CO) using a X40 oil objective (numerical aperture 1.3). Photoactivation was performed by applying 50% 405 laser for 1 msec / per pixel laser for 11 iterations to a specified ROI.

Dextran injection

Embryos were injected with HiLyte 488-Tubulin as described in main methods. At 128 cell stage, embryos were dechorionized and mounted in an agar chamber with animal pole facing up. One cell was carefully injected with TAMRA Dextran 10,000 MW (20mg/ml in 0.2M KCL, D1816 Invitrogen) by iontophoretic injection. Injected embryo was placed at multi photon upright system and imaged over time (Olympus & Lavision-Biotec custom stand objective 20X, water, N.A 0.5). Time interval 1.5 minutes, 98 Z slices.

Western blot analysis

Injected and control embryos were collected at the indicated times and detached from their chorions using 0.5 mg/ml pronase (p-8811, Sigma Aldrich) in a dish coated with 1% agar. 50 embryos for each sample were collected and washed with ice-cold PBS. Embryos were then deyolked using a P200 pipet tip in ice-cold PBS and washed in ice-cold PBS. Embryos were homogenized in cholate extraction buffer (2% Sodium Deoxycholate, Sigma Aldrich D-6750, in 10mM Tris pH8.0), diluted in sample buffer and boiled (95°C for 5 minutes). Volume equivalent to 10 embryos were loaded in SDS-PAGE. Membranes were stained with the following antibodies: anti-VPS4 (1:1000, Cat # SAB4200025, Sigma-Aldrich), anti-CHMP4B (1:500, ab105767,abcam), anti GAPDH (1:1000, cat # G096, Applied Biological Materials) and rabbit or mouse-peroxidase secondary antibodies (1:10,000, catalog number 715-035-151 or 711-035-152, Jackson ImmunoResearch, West Grove, PA,). Bands intensities were quantified in ImageJ, using gel analysis plug-in.

Analysis of cell shape

To determine changes in cell shape, videos of embryos labeled with HiLyte 488-Tubulin during cycle 10 (MBT) were recorded for 8 time points at 2 minutes intervals. We manually selected cell triplets that included two connected cells and one non-connected cell, while avoiding triplets that included dividing cells in order to avoid quantifying cell shape that result from mitosis. Cell contours were manually annotated and their aspect ratios were calculated for all cells at all timepoints using SlideBook (version 6, Intelligent Imaging, Denver, CO). A cell's aspect ratio is the ratio between its major axis length and its minor axis length and is a measure the cells' elongated morphology. Aspect ratio of 1 indicates a rounded shape while larger values indicate more elongated shapes. We calculated the absolute difference in the aspect ratio between the cell pairs (connected and non-connected) in each triplet for each time point and averaged the absolute difference for each pair over time to reduce measurement noise (Fig S5*B*).

A

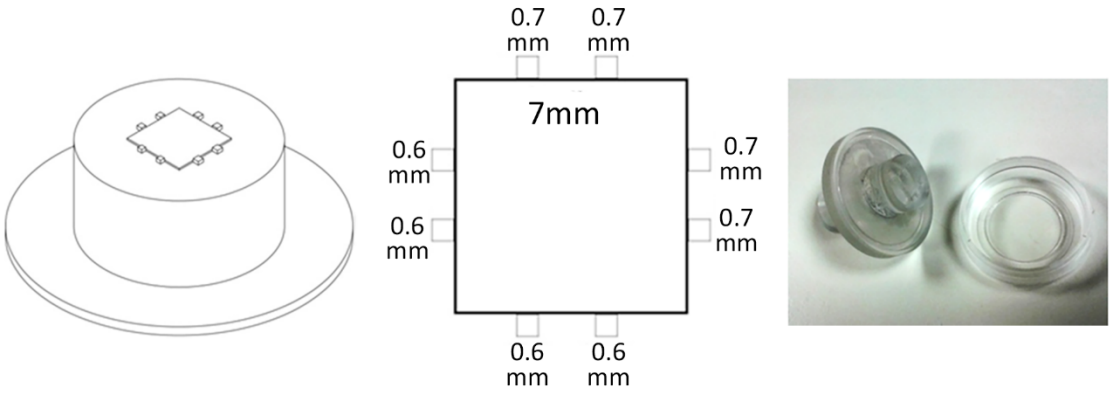

B

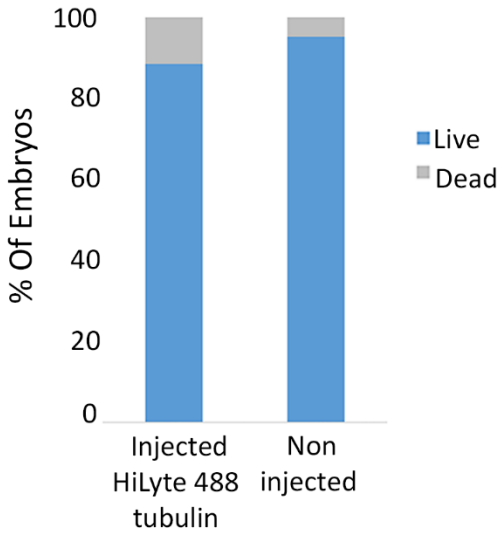

Figure S1: Experimental system

(***A***) Custom-made mold for preparation of agar chambers used for live imaging of zebrafish embryos. Mold was designed according to Wuhr et al (2) to make 8 wells in 0.6-0.7 μm^2 in 35mm glass bottom µ-dish. Chambers were prepared as described in materials and methods. (***B***) Survival of embryos injected or not injected at one-cell stage with HiLyte 488-Tubulin and phenol red was examined 24 hours post fertilization. Injected embryos, 88.6% survival (n=60 embryos); Non injected embryos, 95.23% survival, n=30 embryos). Moreover, normal fish morphology was observed in injected embryos. These results indicate that the injection protocol of fluorescently labeled tubulin did not affect the overall developmental program of the fish.

A

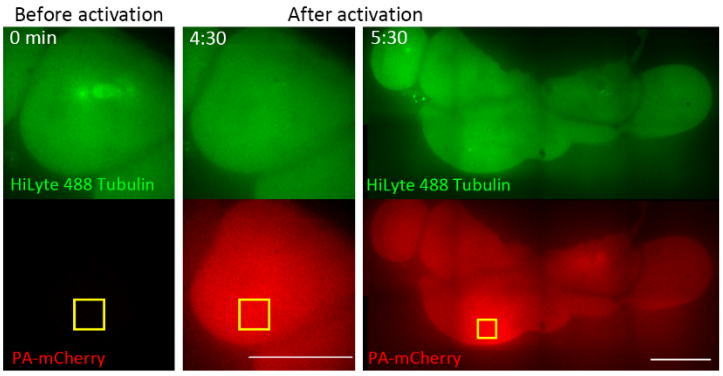

B

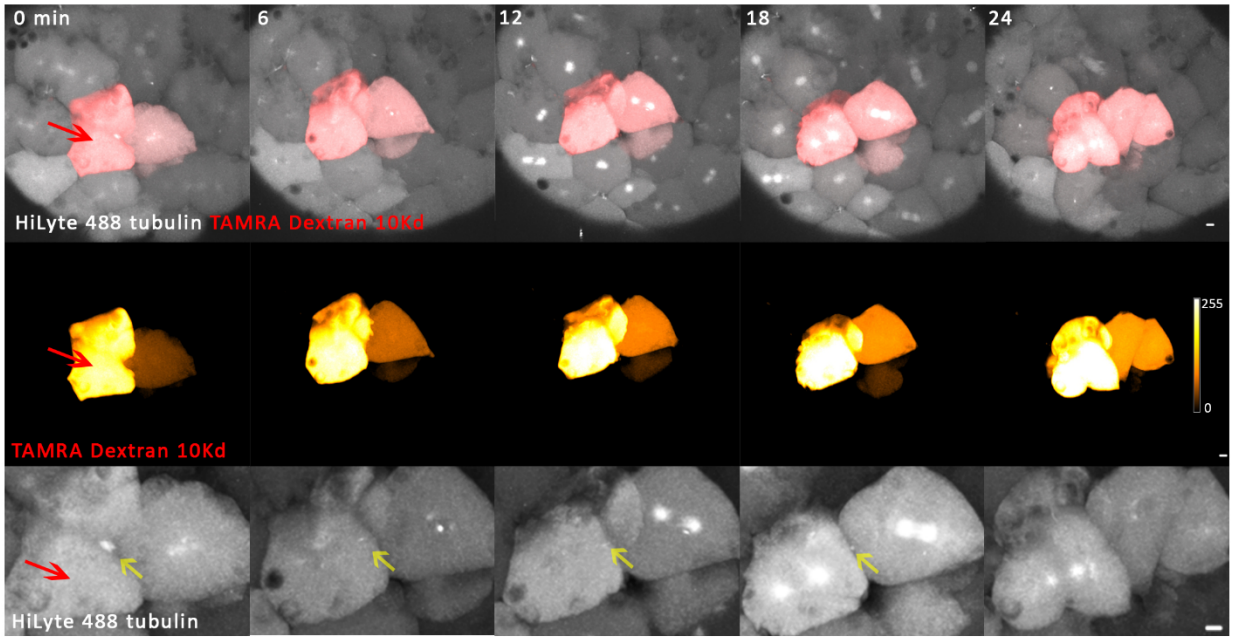

Figure S2: Diffusion between cells in zebrafish embryos

(***A***) PA-mCherry diffused throughout the whole embryo 16-cells stage. Embryo was injected with HiLyte 488- Tubulin (green) and PA-mCherry (red), imaged and photoactivated at 16-cells stages using a spinning disk confocal microscope, as described in sup methods. Shown at single slices from the 3D volume acquisition of a representative embryo. From left to right: zoomed-in image of the photoactivate cell before activation (time 0), zoomed-in image of the photoactivate cell after activation, montage of the whole embryo at 32 cells stage. Yellow squares indicate the ROI used for photoactivation. Note that several minutes post activation the entire embryo exhibited mCherry fluorescence, indicating that activated PA-mCherry was able to diffuse between all cells in the embryo. are activated in the next division cycle. Scale bar, 100 µm. (***B***) 128-cell embryo expressing HiLyte 488-Tubulin was injected with and TAMRA-Dextran,

10,000 MW as described in sup methods. Red arrow represents injection point. Cells were then recorded in 3D using a multi-photon microscope. Shown are maximum intensity projections images of 3D volumes (84 Z slices of 0.7μm) of selected time points, taken from the movie sequence (Movie S5). HiLyte 488-Ttubulin, white; TAMRA Dextran, red. Upper panel, merged images; middle panel, TAMRA-Dextran, color coded by intensity levels; bottom panel, HiLyte-488 Tubulin. Intercellular bridges are marked with yellow arrows. Note that dextran diffuses only between cells connected by intercellular bridges and did not spread to the entire embryo. Scale bar, 10 μm.

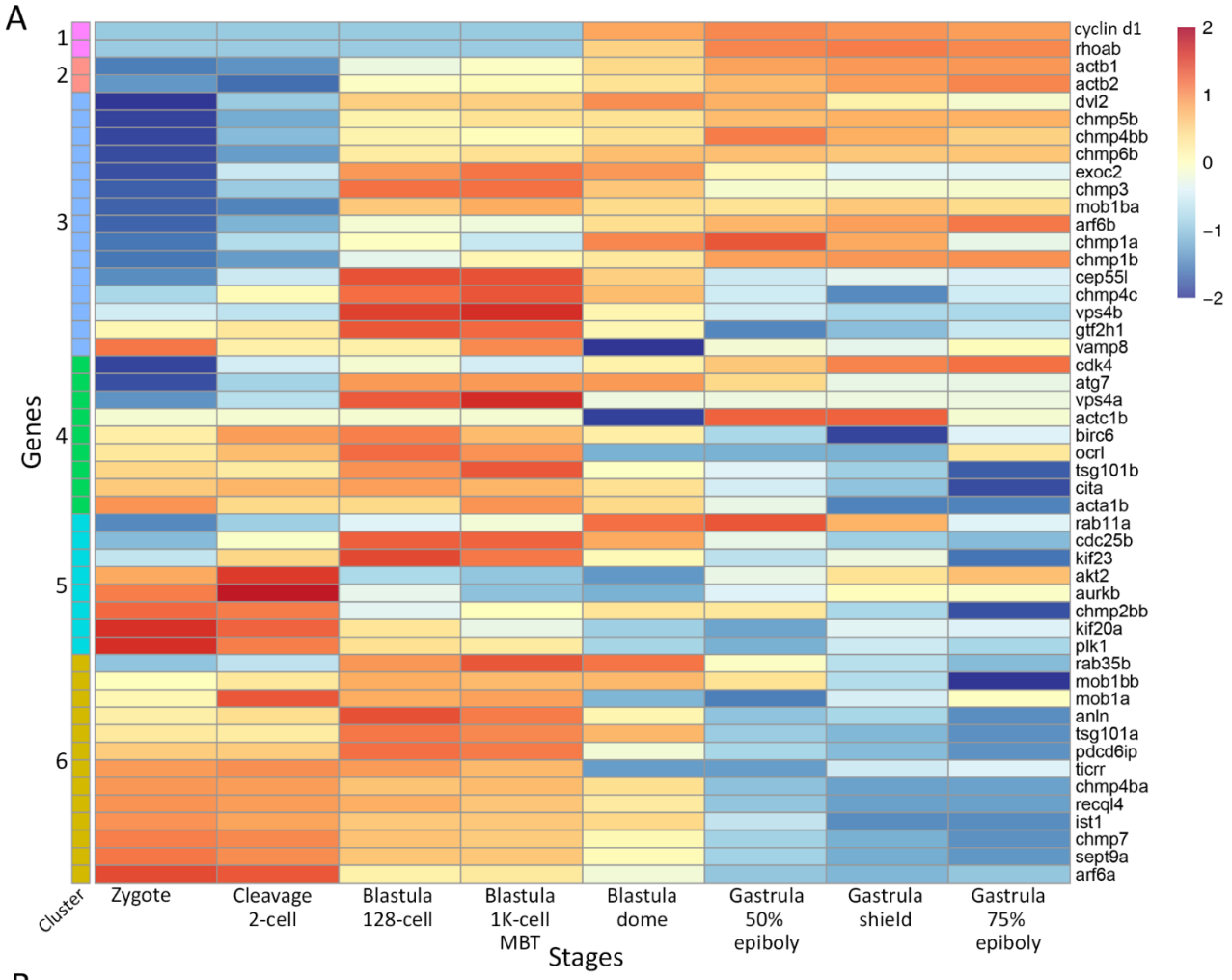
A
Genes
Stages
Cluster
Zygote
Cleavage 2-cell
Blastula 128-cell
Blastula 1K-cell MBT
Blastula dome
Gastrula 50% epiboly
Gastrula shield
Gastrula 75% epiboly
cyclin d1
rhoab
actb1
actb2
dvl2
chmp5b
chmp4bb
chmp6b
exoc2
chmp3
mob1ba
arf6b
chmp1a
chmp1b
cep55l
chmp4c
vps4b
gtf2h1
vamp8
cdk4
atg7
vps4a
actc1b
birc6
ocrl
tsg101b
cita
acta1b
rab11a
cdc25b
kif23
akt2
aurkb
chmp2bb
kif20a
plk1
rab35b
mob1bb
mob1a
anln
tsg101a
pdcd6ip
ticrr
chmp4ba
recql4
ist1
chmp7
sept9a
arf6a
2
1
0
−1
−2

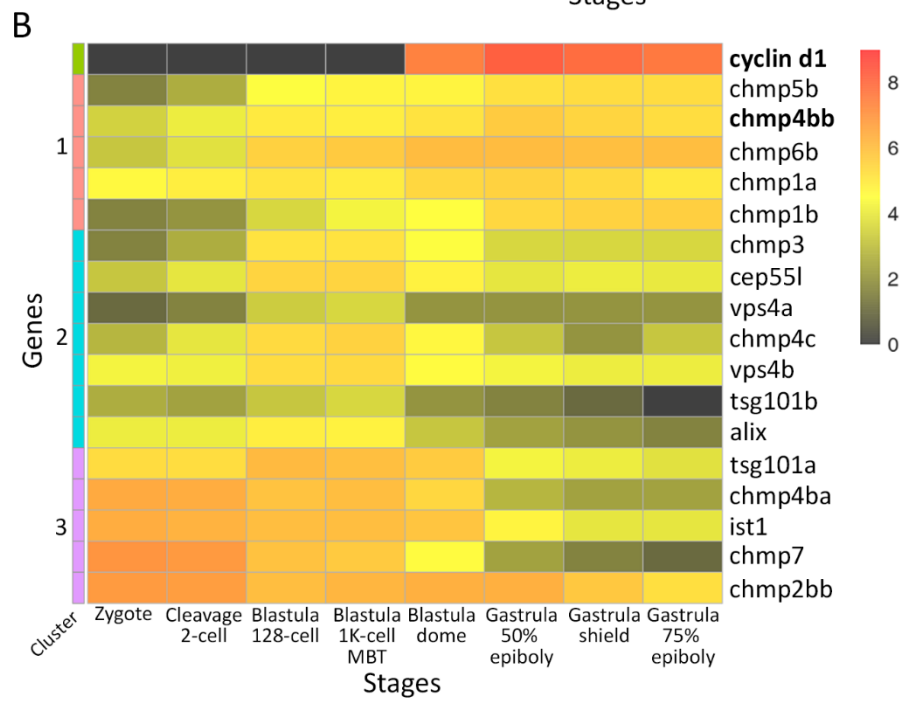
B
Genes
Stages
Cluster
Zygote
Cleavage 2-cell
Blastula 128-cell
Blastula 1K-cell MBT
Blastula dome
Gastrula 50% epiboly
Gastrula shield
Gastrula 75% epiboly
cyclin d1
chmp5b
chmp4bb
chmp6b
chmp1a
chmp1b
chmp3
cep55l
vps4a
chmp4c
vps4b
tsg101b
alix
tsg101a
chmp4ba
ist1
chmp7
chmp2bb
8
6
4
2
0

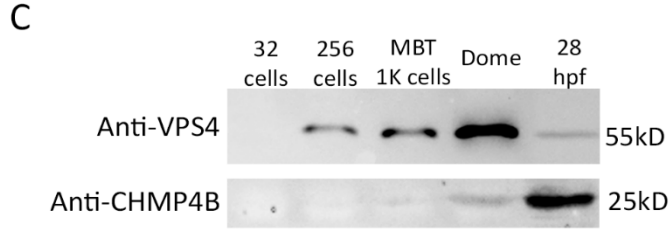
C
32 cells
256 cells
MBT 1K cells
Dome
28 hpf
Anti-VPS4
55kD
Anti-CHMP4B
25kD

Figure S3: mRNA transcription levels of late Cytokinetic related genes at early development

(***A***) RNA-seq profiles of 48 late cytokinetic related genes and *cyclin d1* across eight developmental stages of zebrafish embryos, downloaded from the data based established by White et al. are shown on a heatmap (4). Rows correspond to individual genes and columns correspond to developmental stages. Colors in heatmap indicate the expression levels of each gene across the samples, relative to its mean expression and trimmed to range [−2, 2]. Six clusters (Cluster 1-6, left bar color coding) were identified by hierarchical clustering, clusters were sorted manually, and genes within each cluster were sorted by their presented (relative) expression in the Zygote stage. (***B***) RNA- seq profiles of ESCRT genes (raw data). RNA sequencing data of zebrafish embryos from eight developmental stages is used to present the expression levels of *cyclin d1* and 17 ESCRT genes. Log2-transformed FPKM levels of the genes are presented on a heatmap, genes are sorted according to hierarchical clustering as presented in Fig 3B. Rows correspond to individual genes and columns correspond to developmental stages. Colors represent the expression levels of each gene across the samples [log2(FPKM)]. Expression values are trimmed to range [0, 9]. (***C***) Expression levels of ESCRT proteins at different embryonic stages as determined by western blot analysis. Wild-type embryos were lysed at indicated stages and subjected to western blot analysis using anti-VPS4 and anti-CHMP4B antibodies. Volumes equivalent to 10 embryos were loaded in each lane. The results are in agreement with the data presented in heatmap for mRNA expression. Vps4 is not expressed at 32-cell stage, and its levels gradually increase until dome stage while Chmp4b is not expression prior to MBT (n=3).

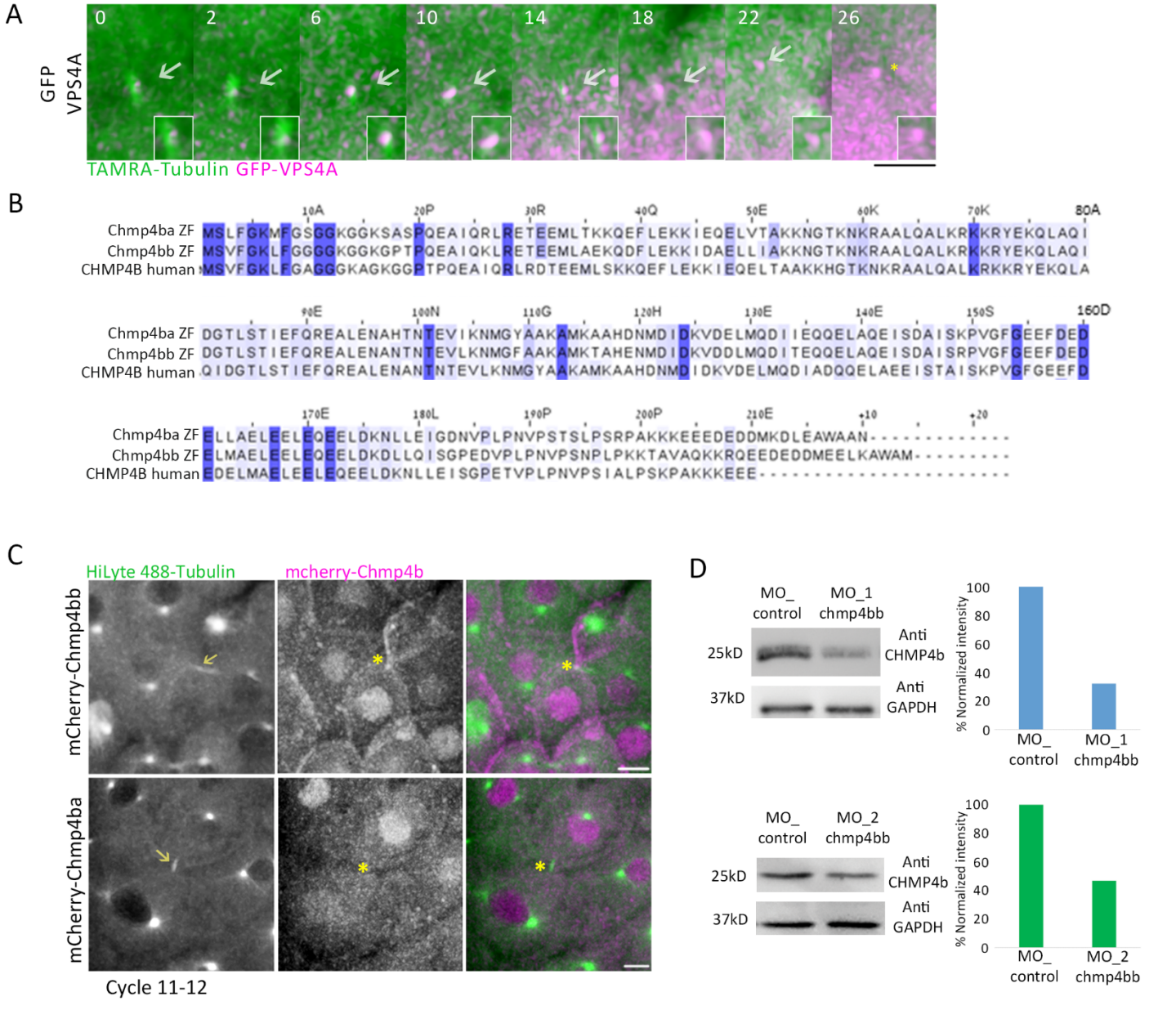
A
GFP VPS4A
0
2
6
10
14
18
22
26
TAMRA-Tubulin GFP-VPS4A
B
Chmp4ba ZF
Chmp4bb ZF
CHMP4B human
C
HiLyte 488-Tubulin
mcherry-Chmp4b
mCherry-Chmp4bb
mCherry-Chmp4ba
Cycle 11-12
D
MO_ control
MO_1 chmp4bb
MO_2 chmp4bb
25kD
37kD
Anti CHMP4b
Anti GAPDH
% Normalized intensity
E
Intercellular bridge duration (minutes)
Cycle
Conrtol
Chmp4bb KD
F
% of Embryos
AB
Dead
Deformed
Live
ns

Figure S4: ESCRT proteins in zebrafish embryogenesis

(***A***) Live imaging of hVPS4 arrival to the intercellular bridge of cells in embryos at blastula stage. Embryos were injected with mRNA that encodes for VPS4A component fused to GFP (magenta) and with HiLyte 488-Tubulin (green). Shown are maximum intensity projection images (10 Z slices of 0.7 µm intervals) taken from a representative cell imaged in embryos at blastula stage. VPS4A localized to the intercellular bridge (gray arrow) and was detected at the midbody remnant post abscission (yellow asterisk). Time 0 represents the time of bridge formation. Zoomed-in images of the midbody are shown as insets in each frame. Data was obtained from two embryos and a total of 10 intercellular bridges. Scale bar 10 µm (***B***) Multiple sequence alignment of human CHMP4B (NP_789782.1), zebrafish Chmp4ba (NP_956489.1) and zebrafish Chmp4bb (NP_998622.1). (***C***) Visualizing the two CHMP4B homologs in cytokinetic cells of zebrafish embryos. Embryos were injected with mRNA that encodes to Chmp4bb (upper panel) and Chmp4ba (bottom panel) fused to mCherry (magenta) and with HiLyte 488-tubulin (green). Shown are maximum intensity projection images (10 Z slices of 0.9-1 µm intervals) taken from a representative cell imaged in embryos at cycle12th. Intercellular bridges are indicated by arrows. Chmp4bb localized to the intercellular bridge while Chmp4ba exhibited diffused pattern and could not be detected at the intercellular bridge (yellow arrow). Scale bar 10µm. (***D)*** Depleting Chmp4bb levels using morpholinos. Embryos were injected with MO_control, MO_1chmp4bb or MO_2chmp4bb, lysed 24 hours post fertilization and subjected to western blot analysis using CHMP4B and GAPDH antibodies. Volume equivalent to 10 embryos was loaded for each treatment. Chmp4bb levels were reduced by 67.9% in MO_1chmp4bb and by 53.4% in MO_2chmp4bb compared to MO_control embryos. MO_1chmp4bb was therefore used for Chmp4bb depletion experiments. (***E***) Duration of intercellular bridges in Chmp4bb depleted embryos. Zebrafish embryos were injected with MO_1chmp4bb oligo and HiLyte 488-Tubulin and intercellular bridges were imaged in embryos at 9th to 12th cycles. Intercellular bridge duration was measured as described in material and methods. Averaged bridge duration in Chmp4bb depleted embryos: 9th cycle, 42.18± 19.9 minutes (n=11); 10th cycle, 40.09±16.82 minutes (n=11); 11th cycle , 33± 7.48 (n=13); 12th cycle, 32.57± 13.34 minutes (n=21). Averaged bridge duration in control embryos: 9th cycle, 34±6.96 minutes (n=8); 10th cycle, 24.11±6.47 minutes (n=9); 11th cycle, 28± 9.56 (n=10); 12th cycle, 31.64±10.88 minutes (n=14). ± indicate S.D. n indicates number of bridges. Data was obtained from 8 embryos. (***F***) Percentage live, deformed or dead embryos were calculated 24 hpf for non-

injected embryos (AB strain) and in embryos injected at one cell stage with the specified construct. AB embryos: 78.49%± 14.84 live, 2.68%±8.9 deformed and 19.05%±15.8 dead (data was obtained from 850 embryos in 12 independent experiments). MO_control: 61.98%± 12.36 live, 6.74%±6.11 deformed and 31.28%±13.59 dead (data was obtained from 399 embryos in 9 independent experiments). MO_1chmp4bb: 29.44%± 23.16 live, 4.35%±4.52 deformed and 66.21%±24.83 dead (data was obtained from 350 embryos in 9 independent experiments). MO_2chmp4bb, 14.92%±13.61 live, 25.98%±9.31 deformed and 59.1%±15.14 dead (data was obtained from 194 embryos in 3 independent experiments). The percentage of dead embryos is not significantly different in AB and MO_control embryos (*t*-test, $t_{0.05,19}$=1.861, *p*=0.0783). The percentage of dead embryos is significantly higher in MO_1chmp4bb and MO_2chmp4bb embryos compared to MO_control injected embryos (*t*-test, $t_{0.05,16}$=3.701, *p*=0.001 and *t*-test, $t_{0.05,10}$=2.999, *p*=0.0067 respectively).

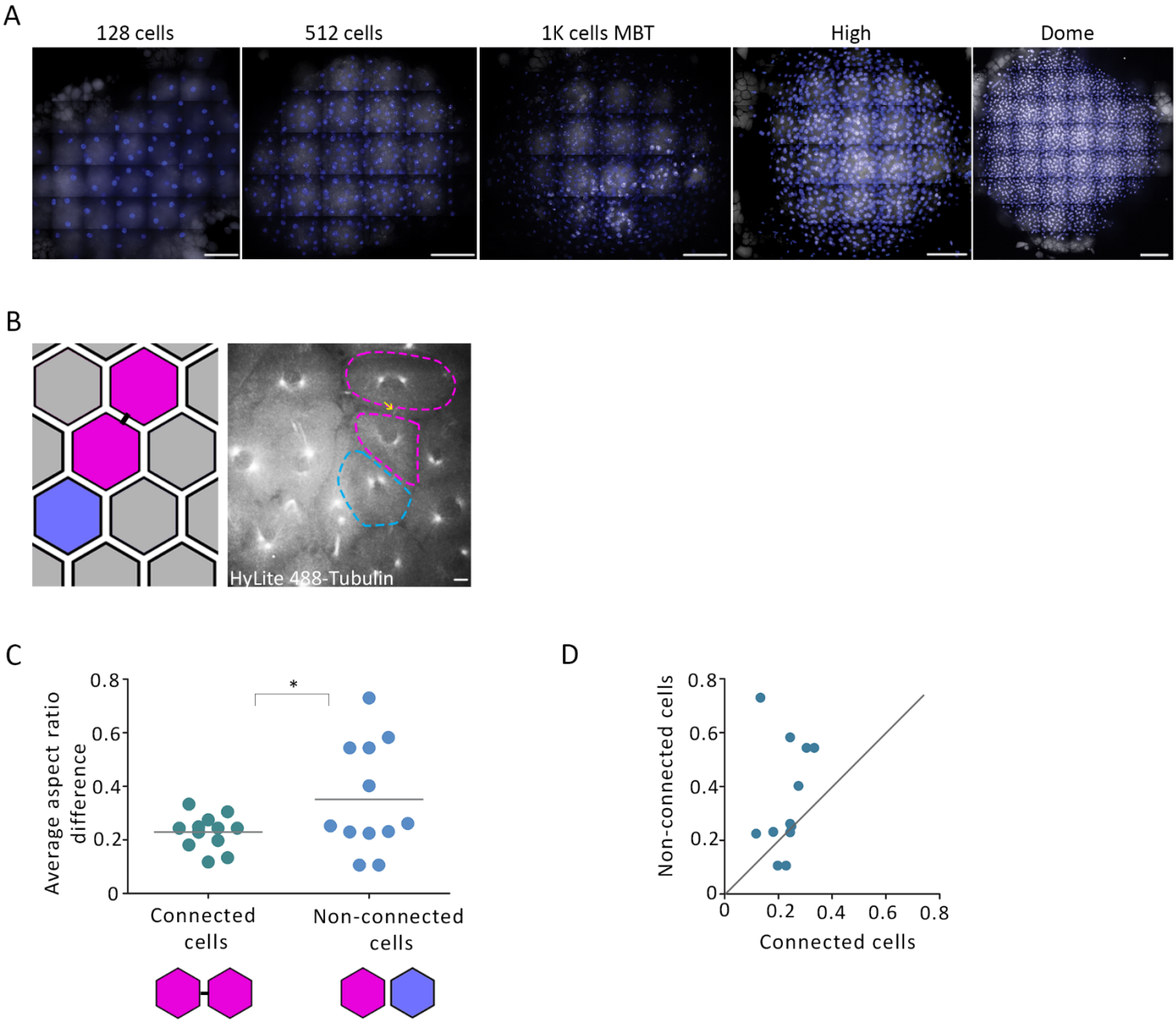

Figure S5: Similarity between connected cells in the embryo

(***A***) Characterizing transcription in zebrafish embryos at blastula stage. Embryos were treated and imaged as described in Fig 4. Shown are nuclear and 5-EU labeling of the entire embryos presented in Fig 4B. Scale bar 100 µm. (***B-D***) quantitative analysis of the similarity in cell shape observed in pairs of cells connected with intercellular bridges and in pairs of non-connected neighboring cells (determined based on Tubulin labeling as described in supplementary methods). (***B***) Representation of the analysis. Cell triplets included one cell pair connected with a bridge (magenta) and another pair with no bridge connection (blue). Left, schematic

representation; right, a representative cell triplet. Scale bar 10μm. (Movie S7) (***C***) The absolute difference in the mean aspect ratio between connected cell pairs (magenta- magenta) non-connected cell pairs (magenta-blue) (*supplementary methods*). The absolute difference in aspect ratios between connected cells 0.23±0.05 was significantly lower than in non-connected neighboring cells (0.35±0.19, *t*-test, $t_{0.05,16}$=1.915, *p*=0.0368). Data was obtained from 5 embryos and total of 12 cell triplets of cells, over 8 time points. (***D***) The matched absolute difference in the aspect ratio between connected cell pairs and their corresponding non-connected pair. The diagonal Y = X is a guide to the eye, match observations above the line indicate larger aspect ratio deviation in non-connected pairs versus their matched connected pair. Wilcoxon matched-pairs signed rank rejects the null hypothesis that the difference between the matched connected- and non-connected pairs is distributed around zero (n=12, Z=-50, *p*=0.026). ± indicate S.D

Table S1. Primers and oligos

Gene	Method	Primer	Restriction enzyme
cep55l zf Fw	Restriction enzyme cloning to mCherry C1 vector	5'-TGTGGAGATCTATGGCGGCGAAGGG-3'	BglII
cep55l zf Rv		5'-TGGCGGGTACCTTAGGTGAAGCAGTAGTCG-3'	KpnI
tsg101 zf FW		5'-TGTGGCTCGAGCTATGGCTGTTGTCAACGAAG-3'	XhoI
tsg101 zf RV		5'-TGGCGGGTACCTCAGTATAGATCACTAAGTCCAGC-3'	KpnI
chmp4bb zf Fw		5'-TGTGGCTCGAGCTATGTCTGTATTCGGCAAATTGTTTGGC-3'	XhoI
chmp4bb zf Rv		5'-TGGCGGGATCCTCACATGGCCCATGCTTTGAGTTCC-3'	BamHI
chmp4ba zf Fw		5'-GCTGCTCTCGAG CTATGTCTTTGTTCGGGAAG-3'	XhoI
chmp4ba zf Rv		5'-GCTGCTGGATCCTTAATTGGCAGCCC-3'	BamHI
GFP Fw	Restriction enzyme cloning to pcs2+ vector	5’-CGTCGTGGATCCAATGGTGAGCAAGGGCGAGGAGC -3’	BamHI
CAAX Rv		5’- GCTGCTTTCGAATCAGGAGAGCACACACTTGCAGCTCATGCAG -3’	BstBI
mcherry Fw	Gibson assembly into pcs2+ vector	5'-GCTACTTGTTCTTTTTGCAGATGGCCTCCTCCGAGGAC-3'	
mcherry-cep55 Rv		5'-TAGAGGCTCGAGAGGCCTTGTTAGGTGAAGCAGTAGTCGAGG-3'	
TSG101 zf OL pCS2 GA RV		5'-TAGAGGCTCGAGAGGCCTTGTCAGTATAGATCACTAAGTCCAGCAGTC-3'	
mcherry-chmp4bb Rv		5'-TAGAGGCTCGAGAGGCCTTGTCACATGGCCCATGCTTT-3'	
mcherry-chmp4ba Rv		5'-CACCGGCGCCTCCGGACTCAGATCTATGTCTTTGTTCGGGAAGATG-3'	
mcherry-chmp4bb Rv		5'-AGTTCTAGAGGCTCGAGAGGCCTTGTTAATTGGCAGCCCAAGC-3'	
MO_1chmp4bb	morpholino oligos for microinjection	5'-ATTTGCCGAATACAGACATATTGTT-3'	
MO_2chmp4bb		5'-AATCCCTGTTTGTCTTCTAGACACC-3'	
MO_standard control		5'-CCTCTTACCTCAGTTACAATTTATA-3'	

Movie S1. Visualizing mitosis in live zebrafish embryos

Embryo was injected with HiLyte-488 tubulin and imaged live during early development (cycles 5-15) using a 20X N.A 0.8 objective to visualize mitosis in the embryo. Maximum intensity projection (30 Z slices at 1 μm) are shown of 4 minutes intervals. Scale bar 10 μm

Movie S2. Visualizing intercellular bridges in live zebrafish embryos

Embryo was injected with HiLyte-488 tubulin and imaged during early development (cycles 9-13) using a 40X N.A 1.3 objective to visualize intercellular bridges at the embryo. Maximum intensity projection (30 Z slices at 1 μm) are shown. Scale bar 10 μm

Movie S3. Intercellular bridge duration

Embryo was injected with HiLyte 488 tubulin (green) and mRNA encoding to mCherry-CEP55 (red) and imaged live using a 40X objective to track the duration of intercellular bridge in the embryo. Maximum intensity projection (29 Z slices at 0.8 μm) are shown. Scale bar 5 μm

Movie S4. Intercellular bridge plasma membrane and microtubules labeling

Embryo was injected with mRNA encoding to CAAX-GFP (red, left) TAMRA-Tubulin (green, middle) and imaged live at the 10^{th} cell-cycle using a 63X objective. Intercellular bridge membrane and microtubules were followed over time. Single Z slice are shown. 2 minutes intervals. Scale bar 10 μm

Movie S5. Persistence of intercellular bridges in early embryos

Embryo was injected with HiLyte 488 tubulin (green) and mRNA encoding to mCherry-CEP55 (red). 1^{st} bridge (white arrow) was formed in the end of cycle 8. At the end of cycle 9, a 2^{nd} bridge (yellow arrow) is formed while the1^{st} bridge was yet to be resolved. Scale bar 10 μm

Movie S6. Dextran diffusion between clusters of cells inter-connected by intercellular bridges

TAMRA-Dextran 10,000 MW (red) was injected to a single cell in a 128 cells embryo that was pre injected with HiLyte-488 tubulin (white). Dextran diffused from the injected cell to cells connected by intercellular bridges but was excluded from neighboring cells. Scale bar 10 μm

Movie S7. Bridge duration in control and Chmp4bb knock down embryos

Embryo was injected with HiLyte 488 tubulin (white) and MO_1chmp4bb and imaged live using a 40X objective to track the duration of intercellular bridge (yellow arrow) in the embryo. Maximum intensity projection (20 Z slices at 1 μm) are shown. Scale bar 5 μm

Movie S8. Changes in cells shape

Tracking cell shape changes in embryos at MBT. White, HiLyte-488 tubulin; Blue, cell masks used for aspect ratio calculations. Scale bar 10 μm

REFERENCES

1. N. Elia, R. Sougrat, T. A. Spurlin, J. H. Hurley, J. Lippincott-Schwartz, Dynamics of endosomal sorting complex required for transport (ESCRT) machinery during cytokinesis and its role in abscission. *Proc Natl Acad Sci U S A* **108**, 4846-4851 (2011).
2. M. Wuhr, N. D. Obholzer, S. G. Megason, H. W. Detrich, 3rd, T. J. Mitchison, Live imaging of the cytoskeleton in early cleavage-stage zebrafish embryos. *Methods Cell Biol* **101**, 1-18 (2011).
3. S. H. Chan *et al.*, Brd4 and P300 Confer Transcriptional Competency during Zygotic Genome Activation. *Dev Cell* **49**, 867-881 e868 (2019).
4. R. J. White *et al.*, A high-resolution mRNA expression time course of embryonic development in zebrafish. *Elife* **6** (2017).